

ESTIMATING THE FREQUENCY AND BANDWIDTH OF SQUARE-SPLIT RING RESONATOR (S-SRR) DESIGNS VIA SUPPORT VECTOR MACHINES (SVM)

Sultan CAN¹ and Gökhan SOYSAL¹

¹Department of Electrical and Electronics Engineering, Engineering Faculty,
Ankara University, Ankara, TURKEY

ABSTRACT. In this study Support Vector Machine (SVM) based estimation technique is proposed for estimating the bandstop frequency and bandwidth of square-split ring resonators. Artificially engineered surfaces especially the planar frequency selective surfaces like the SRRs have narrowband properties so that estimating the filtering frequencies and the bandwidth is essential in a cost and design-effective way. The proposed method, which is superior to optimization methods and 3D electromagnetic solvers in terms of cost and computational burden, achieved accurate results via SVMs generalization capability. This study represents two SVM regression models one for predicting frequency and the other for predicting bandwidth having fast response and accuracy. Results of the proposed model reveal that resonance frequency estimation error, in terms of percentage, is bounded in the interval [0.0542, 3.5938], with an overall error of 0.89 % for the test data. The mean and standard deviation of the percentage error is obtained as 0.9861 and 0.9376, respectively. In addition to that -10dB bandwidth is estimated with the bounded error where estimation error in terms of percentage would be lie in the interval [0.068925, 6.876800] with an overall error of 3.68% for the test data.

1. INTRODUCTION

Isolating electronic devices is crucial not only in terms of electronic device-to-device interaction but also in terms of protecting the body tissue from electromagnetic pollution. Due to the incredible penetration of electronic devices in our daily life, electromagnetic compatibility became a central issue that can be solved by using additional designs such as frequency selective surfaces (FSS), electronic bandgap structures (EBG), left-handed materials, double negative materials (DNG), single negative materials (SNG), and artificial magnetic conductors (AMC) [1,2,12-20]. FSSs are one of the goal-directed components that researchers pay significant

Keywords. Bandwidth estimation, filtering, frequency estimation, machine learning, support vector machine

 sultancan@ankara.edu.tr-Corresponding author; soysal@eng.ankara.edu.tr

 0000-0002-9001-0506; 0000-0002-1397-8564

attention in order with isolation problems [2]. They are periodic arrays of conducting patches or slots on a conducting sheet deposited on a substrate, which behaves as bandpass, and bandstop filters, or absorbers for various frequencies that span up to THz waves from radio waves. Considering the increasingly growing communication systems over the last decades, especially wireless communication allows a striking increase in electromagnetic pollution is on the carpet [1,2]. For all the aforementioned frequency bands restricting unwanted radiation while letting the other signals pass for any system is necessary.

Engineered surfaces are required for filtering the electromagnetic waves and the most familiar one can be regarded as the Split Ring Resonator (SRR) structure. SRR structures, which can be fabricated in different dimensions, are generally fabricated in 2Ds as printed circuit boards by etching the metal element to a dielectric substance. Therefore, an SRR consists of a substrate layer and a patch on the top side of the dielectric substrate. This patch is made of conductive elements, such as gold and copper and they can be designed in several shapes. Due to the advantages in fabrication and implementation, they have received more attention when compared to the 3D versions. Nonetheless, the narrow bandwidth property is an important disadvantage for the proposed structures so that estimating the resonant frequency accurately before manufacturing the design is necessary. Although there are abundant studies performed to find the resonant frequencies in antenna designs, literature is lacking frequency calculation for SRR structures.

Using the 3D electromagnetic solver is one of the most accurate ways to estimate the filtering frequency of the SRR however, the claimer should reconcile the designer to cost, design effort, and computational burden. Another two options, equivalent circuit model and analytical formula for calculating, are cost and time-effective but they are having drawbacks in terms of accuracy. The former is not applicable for higher frequencies since it is not possible to represent such structures with lumped elements at high frequencies and the latter is not accurate because there are no closed-form mathematical expressions for calculating frequency and bandwidth so that optimization will also be a problem due to the lack of mathematical expressions. Among all those techniques for estimating the filtering frequency and bandwidth, Machine Learning (ML) is one of the most preferred ways. Therefore, it is commonly favored by researchers for finding the resonance frequency of RF designs such as antennas. Frequency estimation of FSS is one of the applications that ML can be applied. Supervised and unsupervised learning are the two main approaches that ML can provide. In supervised learning, the aim is to develop a function that maps a set of observations.

In recent years, Support Vector Machine (SVM) applications are becoming more famous and popular in the ML community due to the outstanding performance of the ability of generalization when compared to the traditional methods such as artificial neural network [3-11]. A relatively new supervised non-parametric statistical learning technique, Support vector machines (SVMs), is proposed by Vapnik in 1979 and is based on Vapnik-Chervonenkis theory [3,4]. Therefore, SVM has been implemented into numerous applications such as face detection [3], digit recognition, verification, object detection and recognition, handwritten text detection and categorization [5], speech and speaker verification [6], prediction, etc. Besides those signal applications, it has been used in electromagnetics in microstrip lines [7] and antennas [8,9], filter designs [21], absorber designs [22]. However, to the best of the authors' knowledge, subjects discussing the use of SVM in calculating the properties of SRR are not studied yet.

In this study, a new estimation method is applied to estimate the filtering properties of an S-SRR structure, which is applicable and scalable for several frequency bands. This new estimation technique adopts the SVM regression approach for estimation of the SRR's filtering frequency and -10dB bandwidth by using second-order polynomial kernel and Gaussian kernel-based SVMs respectively, where the minimization problem is solved by utilizing the Sequential Minimization Optimization (SMO) technique. The data set is created by moderate simulate ion runs of 3D EM solver by proposing an SRR structure in 2D geometry. The proposed structure is analyzed in terms of its geometrical and material properties. Impact of substrate thickness, permittivity, copper strip width, slot length, are evaluated regarding the analysis for spanning all possible domains for training. The accuracy of the SVM results is discussed and presented within the paper. SVM approach is conducted considering the filtering frequency f_r and the bandwidth as a function of all those parameters. The results are compared with the 3D solver results and the corresponding error is presented.

2. FREQUENCY AND BANDWIDTH ESTIMATION OF THE S-SRR BY USING SVM

SVM, which is also known as Support Vector Network, used for classification and regression analysis is a good candidate for electromagnetic design problems. Estimating the antenna parameters for a set of training data is one of the application areas in electromagnetics [6-8]. For the given antenna's physical and geometrical parameters, it is possible to estimate antenna operating frequency, bandwidth, and gain parameters. Besides, they are used to estimate the transmission line parameters [7].

In this study, we focused on the frequency and bandwidth estimation of the SRR structure. SVM provides such estimation opportunities in a fast and cost-efficient way. On one hand, considering the full-wave electromagnetic simulators, which are having a burden not only in terms of computation but also in terms of license cost, is a very accurate way of design and optimization. On the other hand, the equivalent circuit model is efficient in terms of cost and quickness. Although equivalent circuit models seem to be a fast model to obtain filtering frequency, it is not an accurate one, especially for high frequencies. Artificial intelligence is getting popular due to its advantages among other methods. As an option ANNs (Artificial Neural Network), which embody traditional empirical Risk Minimization, are candidates for solving such problems; however, they have difficulties in terms of overfitting [10]. On the other hand, a supervised method SVM, which embodies the Structural Risk Minimization principle, are getting popular in the last decades [11]. The generalization capability of SVMs' are superior to ANN is considered in this study and a model is proposed to estimate the band stop frequency and -10dB bandwidth of the square SRR.

Considering a given training data $\{(x_1, y_1) \dots (x_i, y_i)\} \subset \chi \times i$ where i stands for the assembly of real numbers and χ represents the space of input patterns such as $\chi = i^d$ and the goal is to find the function $f(x)$ to approximate the obtained targets y_i for all training data. Here the function $f(x)$ is represented by Lagrange multipliers and Kernel functions, α_i, α_i^* and $K(x_i, x_j)$, respectively as represented in (2.1);

$$f(x) = \sum_{i=1}^l (\alpha_i - \alpha_i^*) K \langle x_i, x_j \rangle + b \quad (2.1)$$

where $\langle \dots \rangle$ stands for dot product in χ and $b \in i$ and $\omega \in i$.

The proposed SVM model approximates the filtering frequencies for the proposed SRR. Those values can be expressed as a function of six SRR parameters as in (2.2) and shown in Figure 1a:

$$f_r = f(x, x_1, w_c, w_s, h_s, \varepsilon_r, h_c) \quad (2.2)$$

Besides the filtering frequency, bandwidth, which is again a function of the structure's physical dimensions and material properties, is crucial in terms of the applications so that it is worth estimating the bandwidth as well as the filtering frequency as in (2.3);

$$BW = g(x, x_1, w_c, w_s, h_s, \varepsilon_r, h_c) \quad (2.3)$$

For performing the estimation, a moderate data set is needed and created by a set of simulations via CST Microwave Studio. The data set is generated by considering all the physical parameters and the material electrical properties and the procedure for the generation of the data set is presented in the next section.

2.1 Data Set Generation

The structure consists of a substrate layer and a patch on the top side of the dielectric substrate having a relative permittivity value of ε_r as shown in Fig. 1a. The side length of the square substrate is denoted as x and the side length of the square SRR is x_1 having a conductor width of w_c and a slot having a width of w_s . The thickness values are h_c and h_s for the conductor and substrate layer, respectively. The resonance frequency of square SRR can be controlled by tuning the capacitance and/or inductance values with the equation $f_r = 1/(2\pi\sqrt{L_{SRR}C_{SRR}})$ where C_{SRR} denoted as the equivalent capacitance and L_{SRR} represent the equivalent inductance values of the SRR. It should be noted that the L_{SRR} and C_{SRR} values, which are depicted in Fig 1b, are the functions of several parameters such as, x_1, w_c, w_s, h_s, h_c and ε_r .

In this section, the filtering frequency of the proposed model is evaluated and analyzed according to its physical and geometrical features via a finite-integration based full-wave electromagnetic solver (CST Microwave Studio) having unit cell boundary conditions. The side length of the conductor ring is one of the physical parameters that affect the L_{SRR} value. The larger conductor lengths cause an increment on the equivalent inductance of the SRR, which causes a decrement in filtering frequency value. To observe the characteristic of the frequency response with a variation of the conductor side length, a set of simulations are conducted via CST Microwave Studio, and the impact of the conductor ring's side length (x_1) on the frequency is given in Fig. 2(a). The shorter conductor side length increases the equivalent inductance so that the frequency has created a blueshift in the frequency. Although the side length of the conductor ring increases the equivalent inductance, the width of the conductor (w_c) shows a quite contrary response (cause a redshift in the frequency) since the increment on the conductor width cause a reduction in the equivalent inductance and also reduction in equivalent capacitance value of the circuit model as shown in Fig. (b).

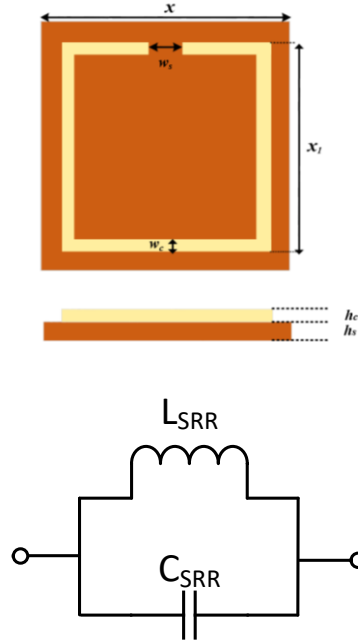


FIGURE 1. Proposed FSS structure (a) geometry (b) equivalent circuit model.

The slot that is created on the conductor loop has a width value of w_s that causes a blueshift with larger values. The variation of the frequency with respect to w_s is presented in Fig. 2(c). Data generation has a set of data regarding the thickness of substrate variation, which can be considered the insignificant effect on filtering bandwidth, but cause a redshift for thicker substrates as presented in Fig. 2(d). The permittivity of the substrate is a parameter that affects the equivalent capacitance where the increase of the permittivity gives a rise in equivalent capacitance of the SRR. Therefore, that frequency decreases with the usage of the high permittivity substrates. The characteristics of the S_{21} with the variation of the permittivity value are given in Fig. 2(e). The Impact of substrate side length (x) is evaluated and the effects are given with the view in Fig. 2(f). It is noteworthy to mention that these changes do not affect the filtering frequency however having a significant effect on bandwidth.

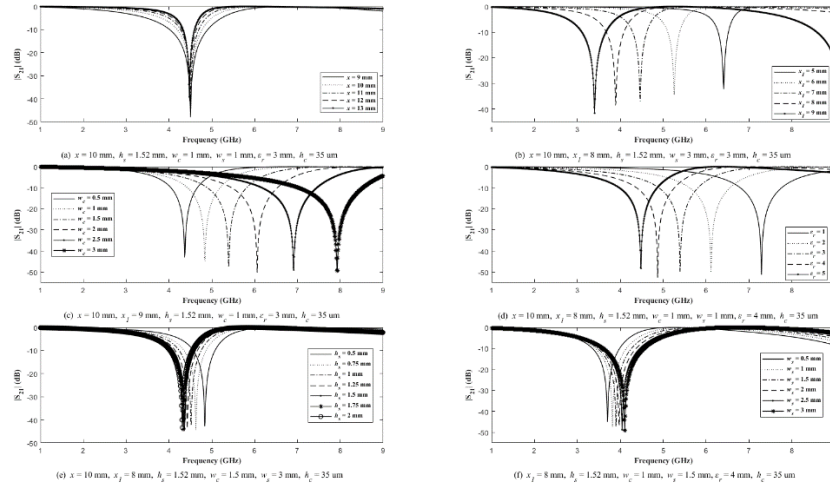


FIGURE 2. Impact of (a) conductor ring's side length (x_1), (b) conductor width (w_c), (c) slot width (w_s), (d) substrate thickness (h_s), (e) permittivity of the substrate (ϵ_r), (f) substrate side length (x).

2.2 Adopted SVM For Estimating Filtering Frequency And Bandwidth of SRR

This study adopts the SVM for estimation of the filtering frequency and -10dB bandwidth of SRR by a polynomial and Gaussian Kernel-based SVM, respectively, which are using SMO (Sequential Minimal Optimization) for solving an optimization problem. The Kernel is a way of computing the dot product of two vectors \mathbf{x} and \mathbf{y} in some very high dimensional feature space so that for estimation selecting the kernel type may affect the accuracy directly. Radial basis function kernel (RBF) in other words Gaussian Kernel, which is one of the most popular Kernel Type, is used among linear, polynomial, and Gaussian Kernels for the adoption of the SVM for the problem.

In this study, parameters of the SVM regression model were optimized to obtain the best model for estimating frequency and bandwidth. Optimization studies have been revealed that training SVM by using second-order polynomial kernel function defined in (2.4) gives the best results for the frequency estimation. Crucial parameters, box constraint, kernel scale, and epsilon have been calculated during the optimization process as 177, 15.557, and 0.002829 respectively. A similar study has been carried out for finding out a suitable model for bandwidth estimation. Studies

have been shown that Gaussian kernel-based SVM provides the best results for bandwidth estimation, and box constraint, kernel scale, and epsilon have been calculated as 990.96, 1.1179, and 0.00026873. Gaussian Kernel can be considered as a function whose value depends on the distance from the origin or some point and can be expressed as in (2.4) and (2.5);

$$K(X_1, X_2) = (1 + X_1 X_2)^2 \quad (2.4)$$

$$K(X_1, X_2) = e^{(-\gamma \|X_1 - X_2\|^2)} \quad (2.5)$$

Where $\|X_1 - X_2\|$ stands for Euclidean distance between points X_1 and X_2 . Data set consists of frequency and bandwidth responses calculated concerning 1134 different values of 7 parameters, x , x_l , w_c , w_s , w_s , h_s , ϵ_r , and h_c . The commercial substrates have two different copper cladding values the 17 μm and 35 μm . Considering the skin depth value which, shows how deeply an RF signal can penetrate a material, both can be used for the desired frequency interval. Skin depth value which depends on the frequency as well as the material's properties such as resistivity and permeability where resistivity, f_0 stands for center frequency for the band of interest, μ_r represents the relative permeability and μ_0 represents the free space permeability. The resistivity values for copper, aluminum, gold, silver, and nickel are 1.678 $\mu\Omega$ cm, 2.6548 $\mu\Omega$ cm, 2.24 $\mu\Omega$ cm, 1.586 $\mu\Omega$ cm, and 6.84 $\mu\Omega$ cm, respectively. Considering the cost copper and aluminum, which have a relative permeability value of ≈ 1 , are two of the most preferred cladding conductor in printed technology. Considering the copper skin depth interval is in between 2.06 μm and 0.652 μm for 1GHz and 10 GHz respectively whilst considering the aluminum cladding options those values are in between 2.59 μm and 0.820 μm for the same frequencies. The commercial cladding option, 35 μm is thicker than the skin depth so that the effect of the thickness can be neglected and the input parameters can be considered as 6 as shown in the figure below.

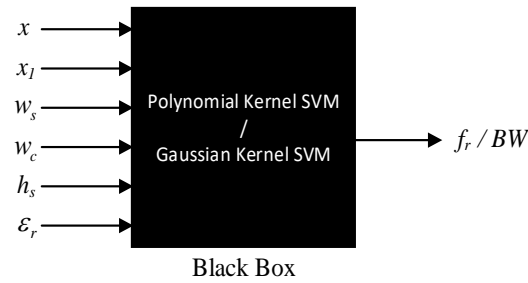


FIGURE 3. SVM illustration as a black box with final input parameters.

Two different SVM regression models have been considered where one of them is for frequency prediction and the other one is for bandwidth prediction. Since the data set is small, both models have been trained by using the whole data set and validation of the SVM regression models has been carried through a k-fold cross-validation procedure. SVM regression models have been tested using new data set generated using a 3D EM solver and frequency and bandwidth predictions obtained by SVM regression models and 3D EM solvers have been compared.

A cross-validation procedure has been performed due to the small training data set. Proposed SVM regression models were validated by performing 5-fold cross-validation by using 1134 sample training data. In this procedure, the training data set is divided into 5 subsets, and one of them is kept as test data and others set to be as training data. SVM regression model is trained using 5 subsets then it is tested using the data hold for the test. This cycle is repeated 5 times where it is guaranteed that each subset is utilized as both test and training data. At each cycle, square error and epsilon loss are calculated and mean values of these parameters are obtained at the end of the validation procedure. Cross-validation results show that the Gaussian kernel-based SVM regression model can be obtained with mean square error 0.00008165 and mean epsilon loss 0.0051172. On the other hand, a second-order polynomial kernel-based SVM regression model can be obtained with a mean square error of 0.04703 and mean epsilon loss of 0.085467.

All the simulations have been performed on Dell Precision Tower 7810 workstation with 10 CPU cores and 32GB RAM. Training phases of Gaussian kernel-based SVN and second-order polynomial kernel-based SVN took 25.23s and 0.81s, respectively.

3. RESULTS AND DISCUSSION

Frequency estimation results presented in Table 1 shows that frequency estimations obtained using the SVM regression model are consistent with the frequencies obtained from the 3D EM solver. Results also reveal that resonance frequency estimation error, in terms of percentage, is bounded in the interval [0.0542, 3.5938], which corresponds to a frequency estimation 144MHz above the true resonance frequency in the worst case. The mean and standard deviation of the percentage error is obtained 0.9861 and 0.9376, respectively. Frequency values belonging to test data and estimated by the SVM regression model have been depicted in Fig.4a. Both frequency estimation error percentages and the results given in Fig. 4a show that the proposed second-order polynomial kernel function-based SVM regression model is a good candidate for the resonance frequency estimation in the SRR having an overall error of 0.89% for 27 different test data given in the table below.

In Table 2, -10dB bandwidth results of the 3D EM solver and SVM regression model have been presented. f_l and f_u represent the upper and lower frequency by which the bandwidth region is defined. A similar discussion can be made for the results presented in Table 2. Bandwidth estimations with the SVM regression model are also consistent with the 3D EM solver results. However, the bandwidth estimation error is greater than the errors obtained in the frequency estimation problem. Since the number of parameters affecting bandwidth is less than those that affect the frequency and we used the same training data set to train the SVM model, the non-informative redundant part of the training data has led to being represented bandwidth with less accuracy. In other words, a small part of the training data set contains information about the relation between design parameters and bandwidth. As a result, it is possible to get more accurate results by changing or expanding the training data set. Bandwidth estimation results are presented in Table 2 and Fig. 4b. Results show that -10dB bandwidth can be estimated with the bounded error where estimation error in terms of percentage would be lie in the interval [0.068925, 6.8768]. Furthermore, the mean and standard deviation of the error percentage has been obtained 3.6828 and 1.8932, respectively. In the worst case, results reveal that bandwidth was being estimated at 105.1 MHz less than the true bandwidth reported by the 3D EM solver. The estimation of bandwidth is conducted with an overall error of 3.68% for the given test data.

TABLE 1. Filtering frequency comparison with 3D EM solver and SVM (units of the dimensions are in mm and frequencies and bandwidths in GHz).

x	Structural Parameters of Square SRR						Frequency		Error %
	x_1	w_c	w_s	h_s	ϵ_r	h_c	3D EM solver	SVM	
10	8	1.5	3	1.52	1	0.035	7.310	7.2057	1.4265
10	8	1.5	3	1.52	2	0.035	6.116	6.1698	0.8801
10	8	1.5	3	1.52	3	0.035	5.386	5.3949	0.1657
10	8	1.5	3	1.52	4	0.035	4.885	4.8810	0.0813
10	8	1.5	3	1.52	5	0.035	4.475	4.6281	3.422
12	8.5	1.5	3	1.52	3	0.035	4.177	6.7159	2.4709
12	9	1.5	3	1.52	3	0.035	3.925	5.6368	1.0001
12	9.5	1.5	3	1.52	3	0.035	3.682	4.7508	1.1014
12	10	1.5	3	1.52	3	0.035	3.475	4.0577	0.4986
12	10.5	1.5	3	1.52	3	0.035	3.277	6.6142	1.3523
12	11	1.5	3	1.52	3	0.035	8.218	6.0082	1.5935
10	8	1	1.5	1.6	3	0.035	4.492	5.4505	0.916
10	8	1	1.5	1.7	3	0.035	4.483	4.9410	0.7442
10	8	1	1.5	1.8	3	0.035	4.465	4.4797	2.4248

10	8	1	1.5	1.9	3	0.035	4.447	4.4952	0.0702
10	8	1	1.5	2.0	3	0.035	4.438	4.4636	0.4318
10	8	1	1.5	1.52	3	0.035	4.510	4.4349	0.6739
10.5	8	1	1.5	1.52	3	0.035	4.501	4.4090	0.8556
11	8	1	1.5	1.52	3	0.035	4.501	4.3858	1.1768
11.5	8	1	1.5	1.52	3	0.035	4.492	4.5224	0.2741
12	8	1	1.5	1.52	3	0.035	4.483	4.4974	0.0804
10	8	0.5	3	1.52	3	0.035	4.366	4.4813	0.4387
10	8	1.0	3	1.52	3	0.035	4.843	4.4740	0.4011
10	8	1.5	3	1.52	3	0.035	5.392	4.4756	0.1658
10	8	2.0	3	1.52	3	0.035	6.076	4.3291	0.8458
10	8	2.5	3	1.52	3	0.035	6.922	4.8186	0.5043
10	8	3.0	3	1.52	3	0.035	7.93	5.3949	0.0542

TABLE 2. Bandwidth comparison with 3D EM solver and SVM (units of the dimensions are in mm and frequencies and bandwidths in GHz).

Structural Parameters of Square SRR									BW		Error %
x	x_1	w_c	w_s	h_s	ϵ_r	h_c	f_i	f_u	3D EM solver	SVM	
10	8	1.5	3	1.52	1	0.035	6.807	7.766	0.958	0.9108	4.925
10	8	1.5	3	1.52	2	0.035	5.616	6.548	0.932	0.8811	5.4603
10	8	1.5	3	1.52	3	0.035	4.889	5.807	0.918	0.8725	4.9559
10	8	1.5	3	1.52	4	0.035	4.3812	5.26	0.882	0.845	4.1905
10	8	1.5	3	1.52	5	0.035	3.979	4.864	0.885	0.838	5.3121
10	5.5	1	1	1.52	3	0.035	6.706	7.039	0.333	0.3402	2.1764
10	6.5	1	1	1.52	3	0.035	5.383	5.752	0.369	0.3837	3.9869
10	7.5	1	1	1.52	3	0.035	4.456	4.897	0.441	0.4672	5.9518
10	8.5	1	1	1.52	3	0.035	3.772	4.339	0.567	0.5509	2.8396
12	7	1.5	3	1.52	3	0.035	6.265	6.751	0.486	0.5168	6.333
12	7.5	1.5	3	1.52	3	0.035	5.653	6.148	0.495	0.5115	3.3246
12	8	1.5	3	1.52	3	0.035	5.122	5.635	0.513	0.5126	0.0689
12	8.5	1.5	3	1.52	3	0.035	4.690	5.230	0.540	0.5227	3.2124
12	9	1.5	3	1.52	3	0.035	4.294	4.852	0.558	0.5333	4.4216
10	8	1	1.5	1.6	3	0.035	4.195	4.744	0.549	0.5554	1.169
10	8	1	1.5	1.7	3	0.035	4.177	4.735	0.558	0.5559	0.381
10	8	1	1.5	1.8	3	0.035	4.717	4.168	0.549	0.5574	1.5266
10	8	1	1.5	1.9	3	0.035	4.699	4.150	0.549	0.5589	1.8084
10	8	1	1.5	2.0	3	0.035	4.690	4.141	0.549	0.5583	1.6926

10	8	1	1.5	1.52	3	0.035	4.197	4.781	0.585	0.5558	4.991
10.5	8	1	1.5	1.52	3	0.035	4.726	4.249	0.477	0.4975	4.3045
11	8	1	1.5	1.52	3	0.035	4.261	4.696	0.435	0.4112	5.4603
11.5	8	1	1.5	1.52	3	0.035	4.654	4.294	0.360	0.3398	5.6173
12	8	1	1.5	1.52	3	0.035	4.298	4.638	0.340	0.3242	4.6402
10	8	0.5	3	1.52	3	0.035	4.033	4.660	0.627	0.5931	5.4016
10	8	1.0	3	1.52	3	0.035	4.431	5.174	0.743	0.7289	1.9044
10	8	1.5	3	1.52	3	0.035	4.901	5.785	0.884	0.8725	1.3003
10	8	2.0	3	1.52	3	0.035	5.480	6.542	1.062	1.0145	4.4726
10	8	2.5	3	1.52	3	0.035	6.207	7.442	1.234	1.2123	1.7772
10	8	3.0	3	1.52	3	0.035	7.009	8.538	1.528	1.4229	6.8768

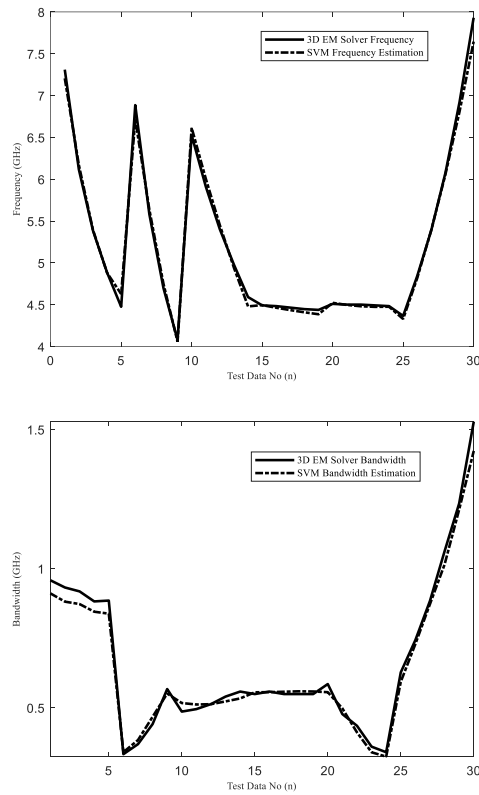


FIGURE 4. SVM and 3D solver comparison for (a) frequency (b) bandwidth.

5. CONCLUSIONS

Results showed that the SVM technique for estimating frequency and bandwidth is preferable due to its generalization capability, fast response, and accuracy. The technique has advantages when compared to 3D electromagnetic solvers, optimization, and other artificial intelligence techniques in terms of license cost, computational burden, and risk minimization. It should be noted that a very good consistency has been achieved in terms of stopband and bandwidth between the 3D solver and SVM regression model by using moderate training data set created via 3D full-wave electromagnetic simulations.

Author Contribution Statements Authors are equally contributed to the paper. All authors read and approved the final copy of the manuscript.

Declaration of Competing Interests The authors declare that they have no known competing financial interests or personal relationships that could have appeared to influence the work reported in this paper.

Acknowledgement This work is supported by the Ankara University Scientific Research Fund (BAP) – BAP Grant Nr: (ÖOP) 21Ö0443002.

REFERENCES

- [1] Can, S., Yilmaz, A.E., Reduction of specific absorption rate with artificial magnetic conductors, *Int. J. RF Microw. Comput. Aided Eng.*, 26 (4) (2016), 349-354. <https://doi.org/10.1002/mmce.20974>
- [2] Munk, B.A., *Frequency Selective Surfaces: Theory and Design*, John Wiley & Sons Inc., New York, 2000.
- [3] Vapnik, V.N., *The Nature of Statistical Learning Theory*, Springer-Verlag, New York, 1995.
- [4] Tsai, H.H., Chang, Y.C., Facial expression recognition using a combination of multiple facial features and support vector machine. *Soft Comput.*, 22 (2018), 4389-4405. <https://doi.org/10.1007/s00500-017-2634-3>
- [5] Aly, S., Mohamed, A., Unknown-length handwritten numeral string recognition using cascade of PCA-SVMNet classifiers, *IEEE Access*, 7 (2019), 52024-52034. <https://doi.org/10.1109/ACCESS.2019.2911851>
- [6] Yaman, S., Pelecanos, J., Using polynomial kernel support vector machines for speaker verification, *IEEE Signal Process. Lett.*, 20 (9) (2013), 901-904. <https://doi.org/10.1109/LSP.2013.2273127>
- [7] Gunes, F., Tokan, N.T., Gurgun, F., Support vector design of the microstrip lines, *Int. J. RF Microw. Comput. Aided Eng.*, 18 (2008), 326-336. <https://doi.org/10.1002/mmce.20290>

- [8] Zheng, Z., Chen, X., Huang, K., Application of support vector machines to the antenna design, *Int. J. RF Microw. Comput. Aided Eng.*, 21 (1) (2011), 85–90. <https://doi.org/10.1002/mmce.20491>
- [9] El Misilmani, H.M., Naous, T., Al Khatib, S.K., A review on the design and optimization of antennas using machine learning algorithms and techniques, *Int. J. RF Microw. Comput. Aided Eng.*, 30 (2020), 22356. <https://doi.org/10.1002/mmce.22356>
- [10] Gunn, S.R., Support vector machines for classification and regression, *SISI Tech. Reports*, 6459, 1998.
- [11] Cortes, C., Vapnik, V.N., Support vector networks, *Mach. L.*, 20 (1997), 73-297.
- [12] Yilmaz, A.E., Kuzuoglu, M., Design of the square loop frequency selective surfaces with particle swarm optimization via the equivalent circuit model, *Radioengineering*, 18 (2) (2009), 95-102.
- [13] Li, J., Li, Y., Cen, Y., Zhang, C., Luo, T., Yang, D., Applications of neural networks for spectrum prediction and inverse design in the terahertz band, *IEEE Photonics J.*, 12 (5) (2020), 1-9. <https://doi.org/10.1109/JPHOT.2020.3022053>
- [14] Qiu, T., Deep learning: a rapid and efficient route to automatic metasurface design, *Adv. Sci. Lett.*, 6 (12) (2019), 1900128. <https://doi.org/10.1002/advs.201900128>
- [15] Alcantara Neto, M.C.A., Oeiras Ferreira, H.R., Leite de Araújo, J.P., Brito Barros F.J., Gomes Neto, A., Oliveira Alencar, M., dos Santos Cavalcante, G.P., Compact ultra-wideband FSS optimized through fast and accurate hybrid bio-inspired multi objective technique, *IET Microwaves, Antennas & Propag.*, 14 (2020), 884-890. <https://doi.org/10.1049/iet-map.2019.0821>
- [16] Chaudhary, V., Panwar, R., FSS Derived Using a New Equivalent Circuit Model Backed Deep Neural Network., *IEEE Antennas Wirel. Propag. Lett.*, 20 (10) (2021), 1963-1967. <https://doi.org/10.1109/LAWP.2021.3101225>
- [17] Bozzi, M., Manara, G., Monorchio, A., Perregrini, L., Automatic design of inductive FSSs using the genetic algorithm and the MoM/BI-RME analysis, *IEEE Antennas Wirel. Propag. Lett.*, 1 (2002), 91-93. <https://doi.org/10.1109/LAWP.2002.805129>
- [18] Chakravarty, S., Mittra, R., Design of a frequency selective surface (FSS) with very low cross-polarization discrimination via the parallel micro-genetic algorithm (PMGA), *IEEE Trans. Antennas Propag.*, 51 (7) (2003), 1664-1668. <https://doi.org/10.1109/TAP.2003.813637>
- [19] Zhu, D.Z., Werner, P.L., Werner, D.H., Design and optimization of 3-D frequency-selective surfaces based on a multi objective lazy ant colony optimization algorithm, *IEEE Trans. Antennas Propag.*, 65 (12) (2017), 7137-7149. <https://doi.org/10.1109/TAP.2017.2766660>
- [20] Ohira, M., Deguchi, H., Tsuji, M., Shigesawa, H. Multiband single-layer frequency selective surface designed by combination of genetic algorithm and geometry-refinement technique, *IEEE Trans. Antennas Propag.*, 52 (11) (2004), 2925-2931. <https://doi.org/10.1109/TAP.2004.835289>

- [21] Monorchio, A., Manara, G., Serra, U., Marola, G., Pagana, E., Design of waveguide filters by using genetically optimized frequency selective surfaces., *IEEE Microw. Wirel. Compon. Lett.*, 15 (6) (2005), 407-409. <https://doi.org/10.1109/LMWC.2005.850482>
- [22] Cui, S., Weile, D.S., Volakis, J.L., Novel planar electromagnetic absorber designs using genetic algorithms., *IEEE Trans. Antennas Propag.*, 54 (6) (2006), 1811-1817. <https://doi.org/10.1109/TAP.2006.875460>